



Cu and Co nanoparticle composites based on starch poly(acrylic acid) hydrogel: reusable catalysts for catalytic reduction of nitrophenol

Massomeh Ghorbanloo^{a,*}, Somaieh Tarasi^a, Roghayeh Tarasi^a, Jun Tao^b

^aDepartment of Chemistry, Faculty of Science, University of Zanjan, 45371-38791 Zanjan, Iran, Tel. +98 24 33054084; Fax: +98 2433052477; emails: m_ghorbanloo@yahoo.com (M. Ghorbanloo), somayehtarasi@yahoo.com (S. Tarasi), tara_2657@yahoo.com (R. Tarasi)

^bState Key Laboratory of Physical Chemistry of Solid Surfaces, Xiamen University, Xiamen, Fujian Province, China, email: taojun@xmu.edu.cn

Received 12 April 2017; Accepted 14 August 2017

ABSTRACT

Starch poly(acrylic acid) (St-p(AA)) hydrogel was synthesized by radical polymerization in solution of starch with acrylic acid as monomer, *N,N'*-methylenebisacrylamide as the cross-linking agent and potassium persulfate as the initiator. St-p(AA) was used as a reactor for in situ synthesis of copper and cobalt nanoparticles. St-p(AA)-Cu and St-p(AA)-Co nanocomposites were characterized by Fourier transform infrared, scanning electron microscopy, transmission electron microscopy, thermal gravimetric analysis and atomic absorption spectroscopy. Catalytic performances of the prepared starch-p(AA)-M (M: Cu, Co) hydrogel composites were investigated by using them as catalyst in the reduction of 4-nitrophenol (4-NP) to 4-aminophenol. The effects of several parameters on the reduction reaction as temperature, catalyst amount and the initial concentration of NaBH₄ were investigated. The activation energy, activation enthalpy and activation of entropy for the reaction were calculated as 36.32, 34.97 and -197.52 J mol⁻¹ K⁻¹, respectively.

Keywords: Nanoparticle; Hydrogel; Starch; Acrylic acid; Nitrophenol

1. Introduction

Recently, metal nanoparticles have been used for many purposes including catalysis [1], reducing agents [2] and so on. Nanoparticles are versatile building blocks with high surface-to-volume ratio, high edge concentration [3], unusual electronic properties [4,5] and high surface energy that make them an interesting subject in CO oxidation [6], alcohol dehydrogenation [7] and nitrophenol reduction [8]. However, the aggregation of these compounds, often poses major barrier against common real-life requests. To overcome these problems, metal nanoparticles are usually loaded or dispersed in a solid matrix, such as polymeric matrices, for example, polysaccharide [9], dendrimers [10], block copolymer micelles [11] and hydrogels [12]. Of these, hydrogels

are highly regarded for using as carrier systems for the in situ synthesis of metal nanoparticles [13,14]. Because their matrixes have the ability to tune the guest–host interaction in order to provide well-defined spatial distribution. The well-defined spatial distribution provides kinetic stability for metal nanoparticles.

Nitrophenol and its derivatives are important by-products produced from pesticides, herbicides and synthetic dyes [15,16]. The reduction of 4-NP to the corresponding amine is also necessary in the industrial synthesis of dyes, drugs, pharmaceuticals, photographic and agricultural chemicals [17]. In addition, this reaction has been widely exploited for confirming the synthesis of efficient nanoparticle catalyst by the study of catalytic activities of nanoparticles [18–21].

In these regards, we prepared starch poly(acrylic acid) (St-p(AA)) hydrogel and used it as reactor as well as stabilizers for the synthesis of copper and cobalt metal nanoparticles. The catalytic activity of the prepared St-p(AA)-M composites

* Corresponding author.

were investigated for the reduction of 4-NP. The effect of different parameters, such as catalyst amount, NaBH_4 amount and temperature, on the reduction reaction was studied. In addition, the reusability of the catalyst was also investigated for five consecutive cycles.

2. Experimental

2.1. Materials and instruments

Cobalt(II) chloride hexahydrate ($\text{CoCl}_2 \cdot 6\text{H}_2\text{O}$, 99% Sigma-Aldrich) and copper(II) chloride (CuCl_2 , 99% Aldrich) were used as metal ion sources while sodium borohydride (NaBH_4 , 98% Aldrich) was used as reducing agent for metal nanoparticle preparation. 2-Nitrophenol (2-NP 99% Acros) and 4-nitrophenol (4-NP 99% Acros) were used as nitro compounds for reduction reaction. Fourier transform infrared (FTIR) spectra were recorded in KBr disks with a Bruker FTIR spectrophotometer. A morphological property of equilibrium swollen St-p(AA) hydrogel was investigated using scanning electron microscopy (SEM) via MIRA3 FEG SEM (Tescan, Czech Republic) and an accelerating voltage of 10 keV. The amounts of metal nanoparticles entrapped in hydrogels were calculated by atomic absorption spectroscopic (AAS) measurements after dissolution of metal nanoparticles embedded within St-p(AA) hydrogel by treating with 5 M HCl aqueous solution. Transmission electron microscopy (TEM, HITACHI S-4800) was used to find out the size of metal nanoparticles inside the hydrogel nanocomposites. To image the copper nanocomposites on TEM, the swollen hydrogel was finely grounded with the help of a soft ball and the resulted hydrogel nanocomposites samples were dispersed in 1 mL of distilled water and dropped on copper net. Thermogravimetric analysis (TGA) was performed on an STA409PC Netzsch thermal analyzer in flowing N_2 (60 mL min^{-1}) at a heating rate of $10^\circ\text{C min}^{-1}$.

2.2. Preparation and characterization of bare St-p(AA) and St-p(AA)-M composites

St-p(AA) hydrogel was prepared according to previous literatures [22]. On average, 12.25 g acrylic acid (AA; 0.17 mol) was partially neutralized with sodium hydroxide solution which was added dropwise in an ice bath. A suspension of 1.00 g starch was added to AA solution and then was stirred for 15 min. On average, 0.05 g of *N,N'*-methylenebis(acrylamide) (MBA) and 1 mL ammonium persulfate solution in water (30% W/V) were added to mixture and polymerization was completed in water bath under nitrogen atmosphere at 70°C for 30 min. The resulting hydrogel was poured into 100 mL acetone and stirred 24 h. Then the sample was oven-dried in an air-circulating oven at 70°C for 24 h.

Selected FTIR (KBr, cm^{-1}): (St-p(AA)): 3,440 (br), 2,929 (m), 2,855 (w), 1,751 (m), 1,648 (s), 1,472 (m), 1,444 (w), 1,395 (m), 1,172 (w), 1,124 (m), 1,034 (m), 810 (w), 684 (m), 668 (s), 660 (w).

A morphological property of equilibrium swollen St-p(AA) hydrogel was investigated using SEM via MIRA3 FEG SEM (Tescan, Czech Republic) and an accelerating voltage of 10 keV. The samples were removed from the water and quickly frozen by immersion in liquid nitrogen. The hydrogels were freeze-dried at -50°C for 3 d to maintain

their porous structure without any collapse. After that, the dried samples were deposited onto an aluminum stub and sputter-coated with gold for 60 s to enhance conductivity.

2.3. Preparation of St-p(AA)-Cu and St-p(AA)-Co composites

For in situ fabrication of metal nanoparticles within St-p(AA) hydrogel, first metal ions (Cu^{2+} or Co^{2+} , separately) were loaded into hydrogel network by dispersing 0.1 g of the dried St-p(AA) hydrogel in 50 mL, 500 ppm aqueous solution of CuCl_2 or CoCl_2 , separately, for 24 h at room temperature under continuous stirring. The metal ion-loaded hydrogels were washed with deionized (DI) water to remove unbound metal ions. Finally, metal ion-loaded and cleaned hydrogel pieces were transferred to 50 mL of 0.5 M aqueous NaBH_4 solution in a water bath shaker at room temperature for 5 h till the reduction process was completed. Again, hydrogels were washed with DI water. To determine the amounts of metal nanoparticles inside St-p(AA) network, St-p(AA)-M composites were treated with 5 M HCl, to dissolve metal particles from the network and the amount of metal nanoparticles released from the composites were determined by atomic absorption spectroscopy.

2.4. General reduction procedure

To reduce 4-NP to 4-AP 50 mL, 0.35 M NaBH_4 containing 0.01 M 4-NP solution was prepared. Then, certain amount of composite hydrogel catalyst was added to the solution to initiate the reduction. After adding the hydrogel-composite catalyst, 0.3 mL sample was taken from the reaction medium at certain time intervals and diluted to certain concentration to observe the conversion of 4-NP to 4-AP at 400 nm in the absorption spectrum of a UV-visible spectrophotometer. Reduction rate constants were calculated by measuring the decrease in intensities of their absorption peaks at 400 nm. The reusability of the catalyst was investigated by using the same catalyst in five consecutive runs of reduction reactions and the hydrogel-M catalysts were washed with DI water before each usage.

3. Results and discussion

3.1. Characterization

The FTIR spectra for starch, AA and starch-p(AA) hydrogel are presented in Figs. 1(a)–(c), respectively. The FTIR spectrum of starch (Fig. 1(a)) displays the O–H stretching absorption in the region of $3,400 \text{ cm}^{-1}$ and the C–H stretching at $2,935$ and $2,892 \text{ cm}^{-1}$. A triplet peak of starch for the C–O–C stretching appears at $1,170$, $1,100$, and $1,000 \text{ cm}^{-1}$ [23]. In the spectrum of St-p(AA) (Fig. 1(c)) two peaks at $2,929$ and $2,860 \text{ cm}^{-1}$ correspond to the C–H symmetric and asymmetric stretching of starch and MBA. C=O stretching band of AA appears at $1,751 \text{ cm}^{-1}$, and the COO^- stretching of AA appears at $1,444 \text{ cm}^{-1}$. The peaks of starch for the C–O–C stretching appear in the spectrum of St-p(AA) ($1,172$, $1,124$ and $1,034 \text{ cm}^{-1}$) with a shift from what have been described in spectrum of starch [24]. In addition, the NH band of MBA is overlapped by OH peak at about $3,200 \text{ cm}^{-1}$ so the related peak is disordered.

SEM technique was used to analyze the morphology of hydrogel. The SEM image of St-p(AA), shown in Fig. 2, indicates the formation of homogeneous and highly porous material.

The thermal stability of bare hydrogel and nanocomposites were determined by TGA. Fig. 3 shows TGA curves of bare St-p(AA) (Fig. 3(a)) and St-p(AA)-M composites (Figs. 3(b) and (c)). It could be seen clearly that there were two processes of weight loss for all samples when heating up the temperature. The first stage at less than 250°C was due

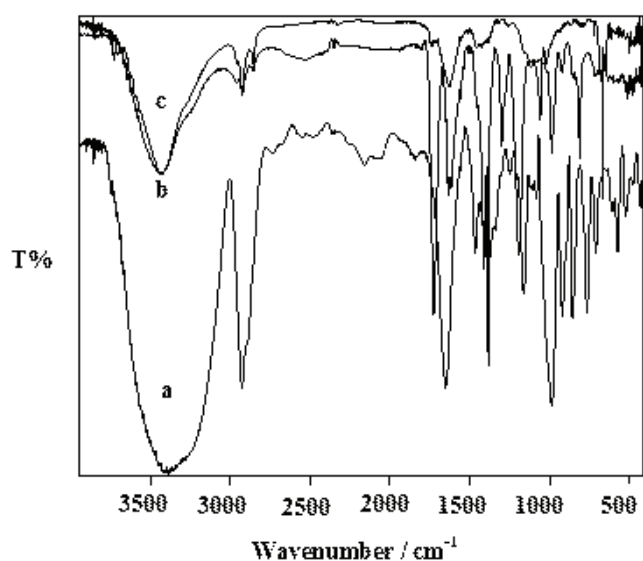


Fig. 1. FTIR spectra of (a) starch, (b) acrylic acid and (c) St-p(AA) hydrogel.

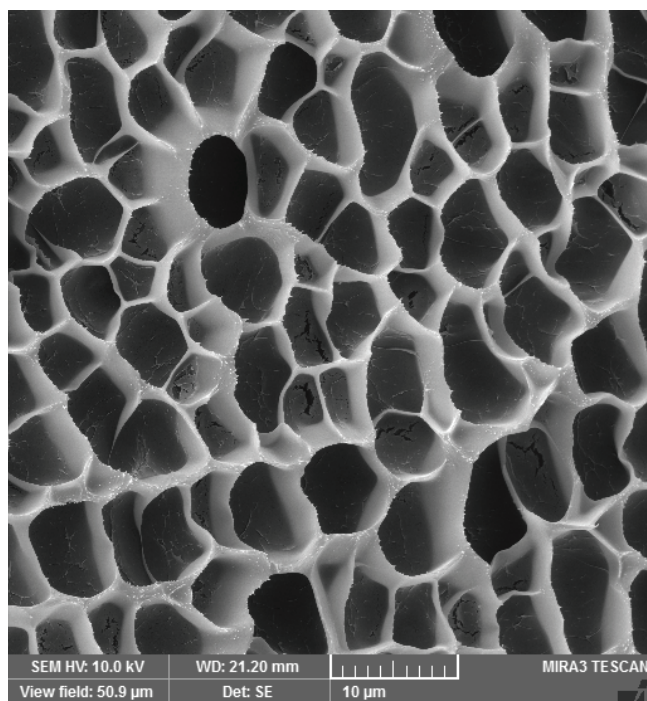


Fig. 2. FESEM image of St-p(AA) hydrogel porous.

to the release of the physically absorbed water. The second as a major weight loss in the range of 250°C–800°C was obtained from the decomposition of St-p(AA). St-p(AA) was thermally decomposed completely with no carbon residue at 800°C, which is similar to other previous reports [25]. Upon their comparison and reduction of bare St-p(AA) hydrogel from St-p(AA)-Cu and St-p(AA)-Co composite hydrogels, it was found that the metal content of the composites was 27 wt% Cu and 43 wt% Co compounds, respectively.

To investigate the nanostructures, the samples were examined with TEM observations. The TEM images of metal nanoparticles-containing St-p(AA) hydrogels are given in Figs. 4(a) and (b). As can be seen, metal nanoparticles with a uniform spherical shape are distributed within St-p(AA) hydrogel matrices. The amount of metal nanoparticles within the hydrogels was determined by using AAS after dissolution by HCl treatment and their amounts are 4.15 and 7.19 mmol g⁻¹ hydrogel for copper and cobalt nanoparticles, respectively.

3.2. Catalytic reduction of 4-NP by Cu(0) and Co(0)-containing St-p(AA)

Catalytic activity of the prepared St-p(AA)-M (M = Cu, Co) composites was investigated for reduction of 4-NP. Nitro compound reduction reactions were elected because of their importance in the environments, and in the number of manufacturing of various pharmacology products, dye and pigment industries [26,27]. According to thermodynamic studies, the reduction of nitro compounds is possible in the presence of excess amounts of aqueous solution of NaBH₄ as reducing agent, with large kinetic barrier [28–30]. Fortunately, the presence of a catalyst helps to overcome this energy barrier and makes these reactions feasible under mild conditions such as room temperature. In all the catalytic reduction of 4-NP, 0.085 mmol of hydrogel-M composite was used as catalyst.

Reduction of nitro compound was tracked by measuring the decrease in their absorbance peak in UV-Vis spectra taken at various intervals of times as shown in Fig. 5.

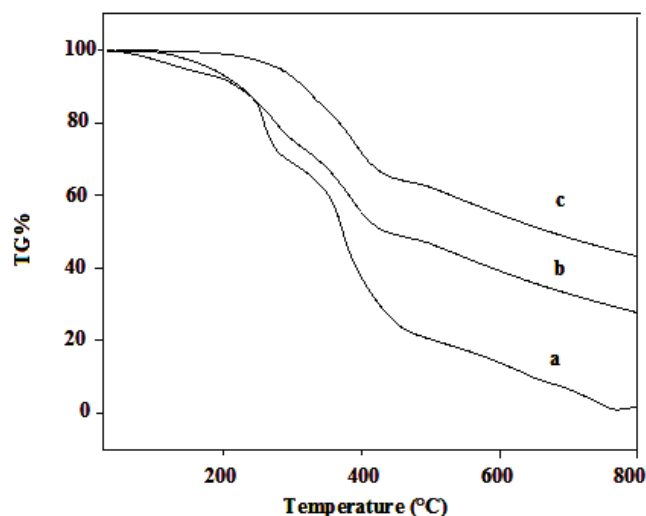


Fig. 3. TG thermograms of (a) bare St-p(AA) and (b) St-p(AA)-Cu (Cu = 27wt%), St-p(AA)-Co (Co = 43 wt%) composites.

The effect of the types of metal nano-catalysts is demonstrated in Fig. 6(a). As illustrated in Fig. 6(a), St-p(AA)-Cu composite reduced 4-NP faster than Co-containing composite; hence, St-p(AA)-Cu composite was selected as catalyst for the detailed kinetic studies.

As degradation of NP was carried out in large excess of NaBH_4 , this reaction was supposed as pseudo-first order and values of k_{app} were calculated by plotting C_t/C_0 vs. time as shown in Fig. 6(b). In order to evaluate the effect of temperature on the catalytic activity of St-p(AA)-Cu composite, the reduction of 4-NP was investigated at three different temperatures; 25°C, 40°C, 60°C keeping the amount of reactant and catalyst constant. Dependence of reaction

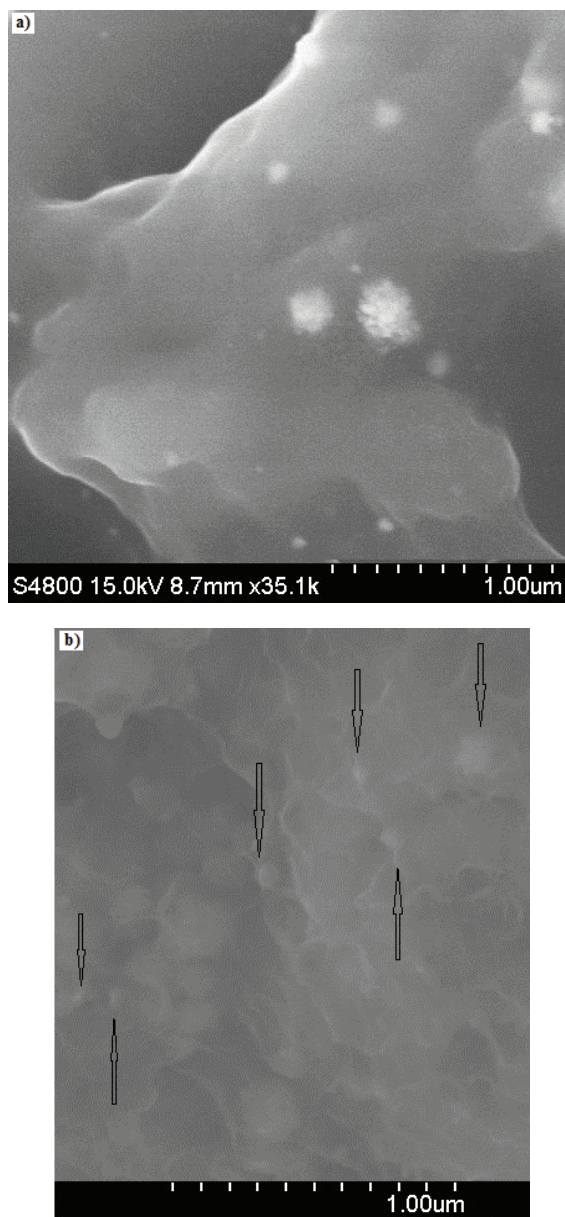


Fig. 4. TEM images of metal nanoparticles from (a) St-p(AA)-Cu and (b) St-p(AA)-Co nanocomposites (white spots considered as Cu nanoparticles in (a) and Co nanoparticles are marked by arrows in (b)).

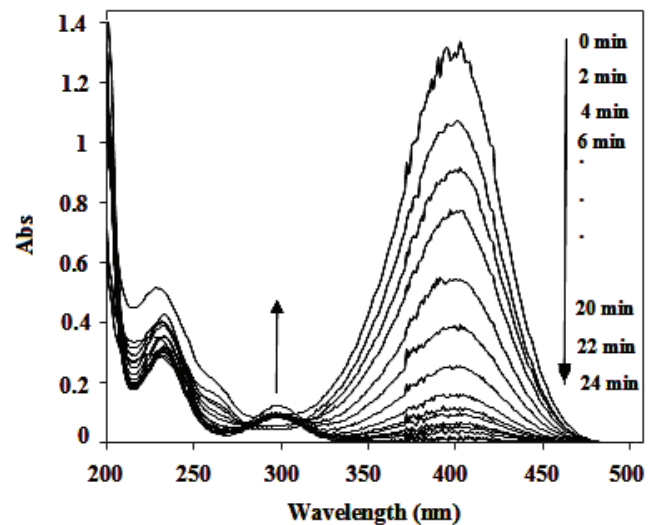


Fig. 5. Reduction of 4-nitrophenol by NaBH_4 ; UV-visible spectra of solution of 4-NP measured at different time in the presence of St-p(AA)-Cu composites at 25°C. Reaction conditions: 0.01 M 4-NP, 0.35 M NaBH_4 , 0.085 mmol of Cu nanoparticle at 25°C.

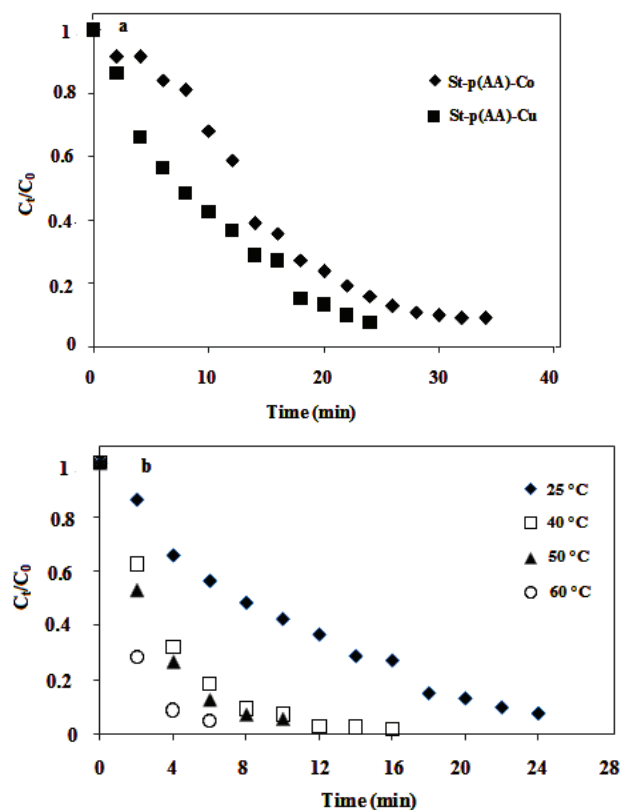


Fig. 6. (a) Plots of C_t/C_0 as a function of time for the reduction of 4-NP catalyzed by St-p(AA)-M (M = Cu and Co) composites at 25°C; (b) plots of C_t/C_0 as a function of time for the reduction of 4-NP catalyzed by St-p(AA)-Co composites at different temperatures. Reaction conditions: 0.01 M 4-NP, 0.35 M NaBH_4 , 0.085 mmol of Cu nanoparticle at 25°C.

rate on temperature is displayed in Fig. 6(b), $((C_i/C_0)$ vs. time at different temperatures) where C_0 is the initial concentration of 4-NP and C_i is the concentration of 4-NP at different time intervals during the reduction reaction. The reduction rates were increased as temperature rise. Because at higher temperature, rate of diffusion of reactant molecules into hydrogel composites and collision frequency of reactant and catalyst increase due to enhance in the average kinetic energy of molecules.

The pseudo-first-order rate constants (k) for the reactions of 4-NP were calculated and are listed in Table 1. The activation energy (E_a) for 4-NP reduction catalyzed by St-p(AA)-Cu was calculated using the well-known Arrhenius equation (Eq. (1)) and it was found as $36.32 \text{ kJ mol}^{-1}$.

The activation enthalpy (ΔH^\ddagger) and entropy (ΔS^\ddagger) were calculated by using Eyring equation (Eq. (2)) and their values were found as $\Delta H^\ddagger = 34.97 \text{ kJ mol}^{-1}$ and $\Delta S^\ddagger = -197.52 \text{ kJ mol}^{-1}$; and their individual constructed $\ln k$ vs. $1/T$, and $\ln(k/T)$ vs. $1/T$, graphs are shown in Figs. 7(a) and (b), respectively.

$$\ln k = \ln A - (E_a/RT) \quad (1)$$

$$\ln k/T = \ln (k_b/h) + \Delta S^\ddagger/R - \Delta H^\ddagger/R (1/T) \quad (2)$$

The effect of catalyst amount on the reduction rate of 4-NP was also investigated. The reaction was done using different amounts of catalyst namely, 0.085, 0.043 and 0.17 mmol. It is clear that the increase in the amount of catalyst has a great effect on the reduction rate, as shown in Fig. 8. The reduction reactions were also carried out in the absence of catalyst. No reduction was detected for 4-NP in the UV-Vis spectrum. This is in agreement with the reported literatures which states that the reduction of 4-NP is thermodynamically unfavorable in the absence of catalyst [31]. To detect whether the reduction rate affected by empty hydrogel or not, the same reaction conditions were organized at 25°C with bare hydrogel, and no reduction was detected.

In order to investigate the effect of NaBH_4 amount on the reduction rate, different amounts of NaBH_4 (0.1–0.5 M) were used in reduction of 4-NP to 4-AP. There is a linear increase in the reduction rate of 4-NP with the increase in the amount of NaBH_4 at 25°C . The same trend has been reported in several literatures [32]

The reusability of St-p(AA)-Cu catalyst systems were also studied by using the catalysts in 4-NP reduction successively up to five times. The percent activity and conversion are reported in Table 2. Activity was calculated by taking ratio

Table 1

The change in the reduction rate constants of 4-NP with different temperatures and activation parameters in catalysis with St-p(AA)-Cu composite

Temperature ($^\circ\text{C}$)	K_{app} (min^{-1})	R^2	ΔH^\ddagger (kJ mol^{-1})	ΔS^\ddagger ($\text{J mol}^{-1} \text{K}^{-1}$)
25	0.208	0.977		
40	0.352	0.980	34.97	-197.52
50	0.594	0.982		
60	1.012	0.974		

of reduction rate of every consecutive reaction to the initial reduction rate, and as reported in Table 2, 100% conversion of 4-NP was observed after 5th use of Cu nano-catalyst systems. However, 4.5% loss in the activity of St-p(AA)-Cu catalysts was observed at the end of four consecutive uses. It can be concluded that these composites can be used up to five cycles without any significant loss of conversion and very little loss of activity in the reduction of 4-NP. The slight decrease in

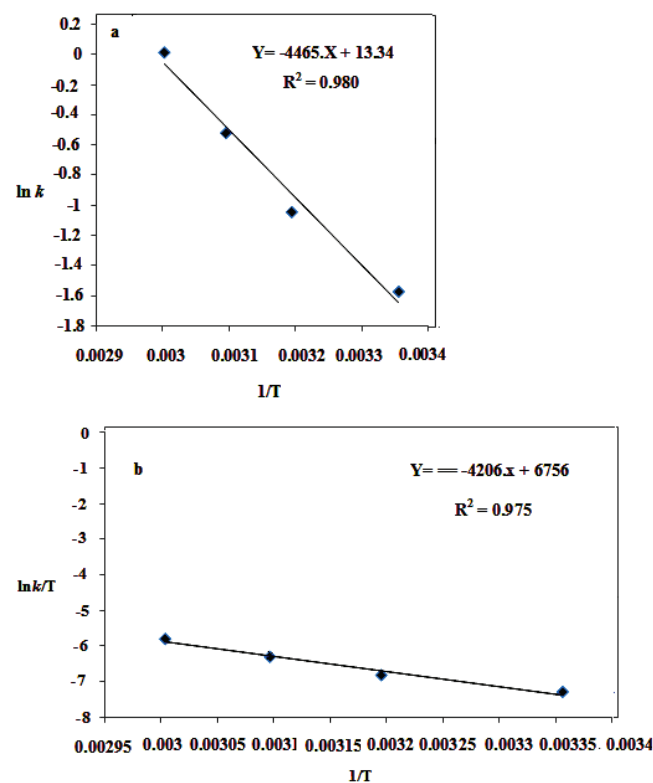


Fig. 7. (a) $\ln k - 1/T$ graphs for 4-NP (Arrhenius Eq. (1)), and (b) $\ln(k/T) - 1/T$ graphs (Eyring Eq. (2)) by St-p(AA)-Cu composites. Reaction conditions: 0.01 M 4-NP, 0.35 M NaBH_4 , 0.085 mmol of Cu nanoparticle at 25°C .

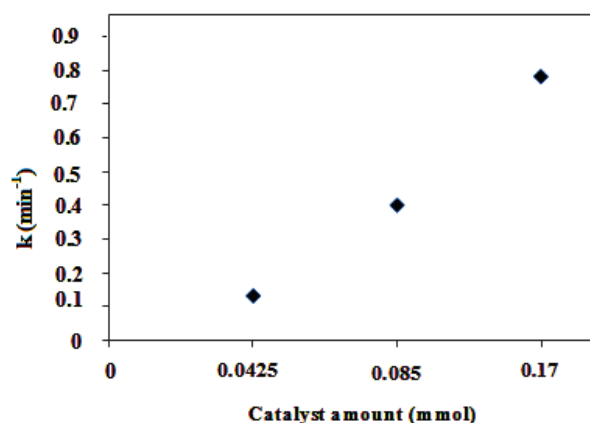


Fig. 8. The change of reduction rate constant of 4-NP with amount of St-p(AA)-Cu as catalyst. Reaction conditions: 0.01 M 4-NP, 0.35 M NaBH_4 , 0.085 mmol of Cu nanoparticle at 25°C .

Table 2

The activity and conversion values of reduction of 4-NP in the presence of St-p(AA)-Cu

Catalyst	Values (%)	Fresh	1th recycle	2nd recycle	3rd recycle	4th recycle	5th recycle
St-p(AA)-Cu	Activity	100	100	97	92	86	82
	Conversion	100	100	100	100	100	100
St-p(AA)-Co	Activity	100	98	90	85	78	69
	Conversion	100	100	100	100	100	100

Table 3

Comparison of the rate constant and activation energy calculated in the present work with reported literature

Catalyst	K_{app} (min ⁻¹)	E_{act}	Reference
p(AMPS)-Cu hydrogel composite	0.1032	28.2	[34]
p(APTMAcI)-Cu	0.405	47.90	[35]
p(AMPS)-Co	0.12	27.8	[36]
CPL-Ag NCs	0.9	Not reported	[37]
Ag@MWCNTs-polymer	0.472	Not reported	[38]
St-p(AA)-Cu	0.208	36.32	This work

the activity can be attributed to the formation of some boron compound and/or some oxides that prevent catalytic performance of active sites [33].

3.3. Comparison with other reported catalytic system

Table 3 provides a comparison of the 4-NP reduction results obtained (k_{app} and E_a) for our present catalytic system with those reported in the literatures [34–38]. From Table 3, it is seen that St-p(AA)-Cu showed higher catalytic activity over reported catalysts. Although p(AMPS)-Cu, and p(AMPS)-Co hydrogel composites showed high reaction rate in 4-NP reduction. A comparison between our catalysts and previously reported systems indicated that our system has higher catalytic activity. One reason for the high catalytic activities in our system could be the softness, flexibility and hydrophilic nature of the hydrogels, carriers and stabilizers, which were used for the preparation of the metal nanoparticles. The other reason could be the hydrophilicity and types of functional groups in the polymeric network, which promotes the overall catalytic process in the system.

4. Conclusion

Herein, it was demonstrated here that a facile preparation of St-p(AA) hydrogel by radical polymerization was accomplished. Starch due to its non-toxicity, good biocompatibility, biodegradability and bioadhesiveness is frequently used for the preparation of nanoparticle matrixes. It was demonstrated that the prepared composites were found very effective catalysts for the individual and simultaneous degradation of nitrophenol. Furthermore, St-p(AA)-Cu composite reduced 4-NP faster than Co-containing composite.

Acknowledgments

Authors are thankful to University of Zanjan for financial support of this study.

References

- [1] S. Wunder, F. Polzer, Y. Lu, Y. Mei, M. Ballauff, Kinetic analysis of catalytic reduction of 4-nitrophenol by metallic nanoparticles immobilized in spherical polyelectrolyte brushes, *J. Phys. Chem. C.*, 114 (2010) 8814–8820.
- [2] S. Sarkar, E. Guibal, F. Quignard, A.K. SenGupta, Effect of particle size and content of the metal on the oxygen reduction by silver-ion exchanger nanocomposites, *J. Nanopart. Res.*, 14 (2012) 715–728.
- [3] A.N. Shipway, I. Willner, Nanoparticles as structural and functional units in surface confined architectures, *Chem. Commun.*, 20 (2001) 2035–2045.
- [4] L.N. Lewis, Chemical catalysis by colloids and clusters, *Chem. Rev.*, 93 (1993) 2693–2730.
- [5] M. Haruta, Size and support-dependency in the catalysis of gold, *Catal. Today*, 36 (1997) 153–166.
- [6] H. Lang, S. Maldonado, K.J. Stevenson, B.D. Chandler, Synthesis and characterization of dendrimer templated supported bimetallic Pt-Au nanoparticles, *J. Am. Chem. Soc.*, 126 (2004) 12949–12596.
- [7] T. Mitsudome, Y. Mikami, H. Funai, T. Mizugaki, K. Jitsukawa, K. Kaneda, Oxidant free alcohol dehydrogenation using a reusable hydrotalcite-supported silver nanoparticle catalyst, *Angew. Chem. Int. Ed.*, 120 (2008) 144–147.
- [8] Ramtenki, V.D. Anumon, M.V. Badiger, B.L.V. Prasad, Gold nanoparticle embedded hydrogel matrices as catalysts: better dispersibility of nanoparticles in the gel matrix upon addition of N-bromosuccinimide leading to increased catalytic efficiency, *Colloid. Surf. A.*, 414 (2012) 296–301.
- [9] J. He, T. Kunitake, A. Nakao, Facile in situ synthesis of noble metal nanoparticles in porous fibers, *Chem. Mater.*, 15 (2003) 4401–4406.
- [10] R.W.J. Scott, O.M. Wilson, R.M. Crooks, Synthesis, characterization and applications of dendrimer-encapsulated nanoparticles, *J. Phys. Chem. B.*, 109 (2005) 692–704.
- [11] B.R. Cuenya, S.H. Baeck, T.F. Jaramillo, E.W. McFarland, Size- and support-dependent electronic and catalytic properties of Au⁰/Au³⁺ nanoparticles synthesized from block copolymer micelles, *J. Am. Chem. Soc.*, 125 (2003) 12928–12934.
- [12] J.H. Kim, T.R. Lee, Hydrogel-templated growth of large gold nanoparticles: synthesis of thermally responsive hydrogel-nanoparticle composites, *Langmuir*, 23 (2007) 6504–6509.
- [13] Y.M. Mohan, K. Lee, T. Premkumar, K.E. Geckeler, Hydrogel networks as nanoreactors: a novel approach to silver nanoparticles for antibacterial applications, *Polymer*, 48 (2007) 158–164.

- [14] Y.M. Mohan, K. Vimala, V. Thomas, K. Varaprasad, B. Sreedhar, S.K. Bajpai, K.M. Raju, Controlling of silver nanoparticles structure by hydrogel, *J. Colloid. Interface Sci.*, 342 (2010) 73–82.
- [15] N. Calace, E. Nardi, B.M. Petronio, M. Pietroletti, Adsorption of phenols by paper mill sludges, *Environ. Pollut.*, 118 (2002) 315–319.
- [16] T. Komatsu, T. Hirose, Gas phase synthesis of paraaminophenol from nitrobenzene on Pt/zeolite catalysts, *Appl. Catal., A*, 276 (2004) 95–102.
- [17] S.U. Sonavane, M.B. Gawande, S.S. Deshpande, A. Venkataraman, R.V. Jayaram, Chemosselective transfer hydrogenation reactions over nanosized γ -Fe₂O₃ catalyst prepared by novel combustion rout, *Catal. Commun.*, 8 (2007) 1803–1806.
- [18] L. Shang, T. Bian, B. Zhang, D.D. Zhang, L.-Z. Wu, C.-Ho Tung, Y. Yin, T. Zhang, Graphene-supported ultrafine metal nanoparticles encapsulated by mesoporous silica: robust catalysts for oxidation and reduction reactions, *Angew. Chem.*, 126 (2014) 254–258.
- [19] R. Brayner, M.J. Vaulay, F. Fievet, T. Coradin, Alginate-mediated growth of Co, Ni, and CoNi nanoparticles: influence of the biopolymer structure, *Chem. Mat.*, 19 (2007) 1190–1198.
- [20] A. Pal, K. Esumi, Photochemical synthesis of biopolymer coated Au core–Ag shell type bimetallic nanoparticles, *J. Nanosci. Nanotech.*, 7 (2007) 2110–2115.
- [21] X. Zhao, Y. Jin, F. Zhang, Y. Zhong, W. Zhu, Catalytic hydrogenation of 2,3,5-trimethylbenzoquinone over Pd nanoparticles confined in the cages of MIL-101(Cr), *Chem. Eng. J.*, 239 (2014) 33–41.
- [22] Q.Z. Yan, W.F. Zhang, G.D. Lu, X.T. Su, C.C. Ge, Frontal polymerization synthesis of starch-grafted hydrogels: effect of temperature and tube size on propagating front and properties of hydrogels, *Chemistry*, 12 (2006) 3303–3309.
- [23] P. Lanthong, R. Nuisin, S. Kiatkamjornwong, Graft copolymerization, characterization and degradation of cassava starch-g-acrylamide/itaconic acid super absorbents, *Carbohydr. Polym.*, 66 (2006) 229–245.
- [24] M. Irani, H. Ismail, Z. Ahmad, M. Fan, Synthesis of linear low-density polyethylene-g-poly (acrylic acid)-co-starch/organo-montmorillonite hydrogel composite as an adsorbent for removal of Pb(II) from aqueous solutions, *J. Environ. Sci.*, 27 (2015) 9–20.
- [25] G. Canche'-Escamilla, M. Canche'-Canche, S. Duarte-Aranda, M. Ca'ceres-Farfan, R. Borges-Argaez, Mechanical properties and biodegradation of thermoplastic starches obtained from grafted starches with acrylics, *Carbohydr. Polym.*, 86 (2011) 1501–1508.
- [26] I. Yoshiaki, K. Masa-aki, Determination of phenylenediamine and related antioxidants in rubber boots by high performance liquid chromatography. Development of an analytical method for N-(1-Methylheptyl)-N'-phenyl-p-phenylenediamine, *J. Health. Sci.*, 46 (2000) 467–473.
- [27] T. Swathi, G. Buvaneswari, Application of NiCo₂O₄ as a catalyst in the conversion of p-nitrophenol to p-aminophenol, *Mat. Lett.*, 62 (2008) 3900–3902.
- [28] M. Ajmal, M. Siddiq, H. Al-Lohedanc, N. Sahiner, Highly versatile p(MAc)-M (M: Cu, Co, Ni) microgel composite catalyst for individual and simultaneous catalytic reduction of nitro compounds and dyes, *RSC Adv.*, 4 (2014) 59562–59570.
- [29] R. Contreras-C'aceres, A. S'anchez-Iglesias, M. Karg, I. Pastoriza-Santos, J. P'erez-Juste, J. Pacico, T. Hellweg, A. Fern'andez-Barbero, L.M. Liz-Marz'an, Encapsulation and growth of gold nanoparticles in thermoresponsive microgels, *Adv. Mat.*, 20 (2008) 1666–1670.
- [30] S. Jana, S.K. Ghosh, S. Nath, S. Pande, S. Praharaj, S. Panigrahi, S. Basu, T. Endo, T. Pal, Synthesis of silver nanoshell-coated cationic polystyrene beads: a solid phase catalyst for the reduction of 4-nitrophenol, *Appl. Catal., A*, 313 (2006) 41–48.
- [31] S.K. Ghosh, M. Mandal, S. Kundu, S. Nath, T. Pal, Bimetallic Pt-Ni nanoparticles can catalyze reduction of aromatic nitro compounds by sodium borohydride in aqueous solution, *Appl. Catal. A.*, 268 (2004) 61–66.
- [32] S. Butun, N. Sahiner, A versatile hydrogel template for metal nanoparticle preparation and their use in catalysis, *Polymer*, 52 (2011) 4834–4840.
- [33] N. Sahiner, H. Ozay, O. Ozay, N. Aktas, A soft hydrogel reactor for cobalt nanoparticle preparation and use in the reduction of nitrophenols, *Appl. Catal. B.*, 101 (2010) 137–143.
- [34] N. Sahiner, O. Ozay, Enhanced catalytic activity in the reduction of 4-nitrophenol and 2-nitrophenol by p(AMPS)-Cu hydrogel composite materials, *Curr. Nanosci.*, 8 (2012) 367–374.
- [35] S.U. Rehman, M. Siddiq, H. Al-Lohedan, N. Sahiner, Cationic microgels embedding metal nanoparticles in the reduction of dyes and nitro-phenols, *Chem. Eng. J.*, 265 (2015) 201–209.
- [36] N. Sahiner, H. Ozay, O. Ozay, N. Aktas, A soft hydrogel reactor for cobalt nanoparticle preparation and use in the reduction of nitrophenols, *Appl. Catal. B*, 102 (2010) 137–143.
- [37] J. Lu, Y. Fu, Y. Song, D. Wang, C. Lu, Temperature-dependent catalytic reduction of 4-nitrophenol based on silver nanoclusters protected by a thermo-responsive copolymer ligand, *RSC Adv.*, 6 (2016) 14247–14252.
- [38] S. M. Alshehri, T. Almuqati, N. Almuqati, E. Al-Farraj, N. Alhokbany, T. Ahamad, Chitosan based polymer matrix with silver nanoparticles decorated multiwalled carbon nanotubes for catalytic reduction of 4-nitrophenol, *Carbohydr. Polym.*, 151 (2016) 135–143.